Journal of Organometallic Chemistry 791 (2015) 244–251

Contents lists available at ScienceDirect

Journal of Organometallic Chemistry

journal homepage: www.elsevier.com/locate/jorganchem

Rhodium(I) complexes containing 9,10-phenanthrenequinone-N-substituted thiosemicarbazone ligands: Synthesis, structure, DFT study and catalytic diastereoselective nitroaldol reaction studies

P. Anitha [a], R. Manikandan [a], P. Vijayan [a], S. Anbuselvi [b], P. Viswanathamurthi [a, *]

[a] Department of Chemistry, Periyar University, Salem 636011, Tamil Nadu, India
[b] Department of Chemistry, Sri Sarada College for Women (Autonomous), Salem 636016, Tamil Nadu, India

ARTICLE INFO

Article history:
Received 5 January 2015
Received in revised form
29 May 2015
Accepted 3 June 2015
Available online 6 June 2015

Keywords:
ONS donor ligand
Rhodium(I) complexes
Crystal structure
Henry reaction
Reusability

ABSTRACT

New rhodium(I) complexes [Rh(CO)(L)] (**1**–**3**) were prepared by the reaction of [RhCl(CO)(PPh_3)$_2$] with 9,10-phenanthrenequinone-N-substituted thiosemicarbazones (HL_{1-3}) and characterized by elemental and spectral analyses (IR, UV–Vis, ^{1}H and ^{13}C NMR, ESI-Mass). The structure of the complex, [Rh(CO)(L_1)] (**1**) has been established by single-crystal X-ray diffraction analysis. The structure has also been optimized by DFT method using LANL2DZ basis set. The synthesized complexes used as catalysts for the diastereoselective nitroaldol reaction of benzaldehyde with nitroethane in presence of ionic liquid at room temperature. The optimized catalyst **2** was found efficient in the asymmetric Henry reaction between various aromatic aldehydes and nitroalkane. The reusability of the catalyst was checked up to five catalytic runs. The result shows marginal loss in yield and the product retains the diastereoselectivity. It is believed that this procedure provides an opportunity for facilely synthesize of large amounts of diastereomerically enriched β-nitroalcohol.

1. Introduction

A great number of Schiff base complexes of transition metal ions have triggered wide interest because of their diverse spectra of biological and catalytic properties. In particular, transition metal complexes of typical Schiff bases, like semicarbazones, thiosemicarbazones and hydrazones, present a wide range of biological and catalytic applications [1–8]. Among them, thiosemicarbazones are of much interest because of their simple preparation, excellent complexation of not only transition but also non-transition p-elements, interesting structural characteristics of their complexes, along with the possibility of their analytical application. This has resulted in a large number of papers and several reviews [9–12] that summarized various aspects of the chemistry of these compounds, such as methods of their synthesis, spectral, magnetic, stereochemical, structural and other characteristics. Hence, for the past five years, our group has been mainly focusing on the study of the variable coordination behavior of thiosemicarbazone ligands towards transition metals, as well as the catalytic and biological activities of the resulting complexes [13]. With this background, we have recently started to work on the ligands derived from 1,2-naphthaquinone/9,10-phenanthrenequinone appended with thiosemicarbazone/semicarbazone [14]. Among the transition metal complexes, rhodium complexes have attracted a lot of attention in the last few decades, mainly due to the metal's scope and versatility as homogeneous and heterogeneous catalysts in a large variety of industrial processes [15–18]. These processes include the production of acetic acid via the Monsanto process [19,20] and the commercial production of L-dopa [21] for the treatment of Parkinson's disease. The discovery of the catalytic properties of Wilkinson's catalyst, viz. [RhCl(PPh_3)$_3$] naturally brought about a widespread search for other rhodium complexes with catalytic activity [22,23].

The Henry or nitroaldol reaction is a powerful and atom-economical carbon–carbon bond forming reaction that can be used to create a new stereogenic center at the β-position of nitro functionality [24]. The resulting product of this reaction is a β-nitroalcohol, which is a versatile intermediate in synthetic organic chemistry [25]. The nitro group in the product can further be conveniently converted into several other functionalities to give synthetically and biologically important bi-functional compounds [26]. In complicated synthetic ventures, the Henry reaction will facilitate the combination of two molecular fragments, under mild

* Corresponding author.
E-mail address: viswanathamurthi72@gmail.com (P. Viswanathamurthi).

http://dx.doi.org/10.1016/j.jorganchem.2015.06.004
0022-328X/

conditions with the formation of two asymmetric centers at the new carbon–carbon juncture [27]. Moreover, the reaction also turns out to be a key step in the preparation of some drugs [28,29]. Since Shibasaki's first report on the asymmetric version of nitro-aldol reaction in 1992 [30], then the broad spectrum of transition metal complexes including copper [31], zinc [32], cobalt [33], chromium [34], palladium [35], rhodium [36], ruthenium [37] and rare metals [38] have been developed to the catalytic version of the nitroaldol reaction. However, to the best of our knowledge, no report of rhodium complexes with ONS donor ligands applied to nitroaldol reaction found in the literature.

Hence from the above aspects in mind, herein, we have reported the synthesis, crystal structure, spectral characterization and DFT study of new rhodium(I) complexes containing 9,10-phenanthrenequinone N-substituted thiosemicarbazone ligands with carbonyl as coligand. The new rhodium(I) complexes were subjected to catalytic nitroaldol reaction of various aldehydes with nitroalkane in ionic liquid medium.

2. Experimental

2.1. Materials and methods

All the reagents used were chemically pure and AR grade. The solvents were purified and dried according to standard procedures. The ligands, $HL_{1\text{-}3}$ and starting complex $[RhCl(CO)(PPh_3)_2]$ were prepared according to literature procedures [14b,39]. Microanalyses of carbon, hydrogen, nitrogen and sulfur were carried out using Vario EL III Elemental analyzer at SAIF – Cochin India. The IR spectra of the ligand and their complexes were recorded as KBr pellets on a Nicolet Avatar model spectrophotometer in 4000–400 cm^{-1} range. Electronic spectra of the complexes have been obtained in dichloromethane using a Shimadzu UV – 1650 PC spectrophotometer in 800–200 nm range. ^1H and ^{13}C NMR spectra were measured in Jeol GSX – 400 instrument using $CDCl_3$ as the solvent at room temperature with TMS as the internal standard. The ESI-Mass spectra were recorded by LC-MS Q-ToF Micro Analyzer (Shimadzu) in the SAIF, Panjab University, Chandigarh. HPLC analyses were performed on a SHIMADZU LC-6AD using a chiral column (Phenomenex Chiralpack) with HPLC grade *n*-hexane and isopropanol as solvents. Melting points were checked on a Technico micro heating table and were uncorrected.

2.2. Synthesis of complexes

2.2.1. Synthesis of [Rh(CO)(L_1)] (**1**)

An ethanol solution (10 mL) containing HL_1 (0.1 mmol) was added to $[RhCl(CO)(PPh_3)_2]$ (0.1 mmol) in ethanol (10 mL) and the resulting red color solution was refluxed for 4 h. On cooling the contents to room temperature, the red colored complex separated out. It was filtered off and recrystallized from ethanol. Red colored crystals, suitable for single crystal X-ray diffraction analysis was obtained by slow evaporation of compound in ethanol/chloroform mixture. Yield: 85%; MP: 224 °C; Anal. calc. for $C_{16}H_{10}N_3O_2RhS$ (%): C, 46.73; H, 2.45; N, 10.22; S, 7.80. Found (%): C, 46.56; H, 2.31; N, 10.40; S, 7.67. IR (KBr, cm^{-1}): 1952 (C≡O); 1625 (quinone C═O); 1578 (C═N); 746 (C–S). UV–Vis (λmax, nm): 453, 393, 334, 297. ^1H NMR (400 MHz, $CDCl_3$, ppm): 9.41 (s, 2H, NH_2); 7.26–7.69 (m, 8H, Ar–H). ^{13}C NMR (100 MHz, $CDCl_3$, ppm): 203.87 (C≡O); 180.24 (quinone C═O); 171.82 (C–S); 159.96 (C═N); 125.60, 127.43, 129.58, 131.03, 131.18, 133.40, 133.56, 139.56, 139.89 (Ar–C). ESI-Mass (m/z) = 411.4 [M^+].

2.2.2. Synthesis of [Rh(CO)(L_2)] (**2**)

The synthesis of **2** was carried out by the same procedure as described for **1** with HL_2 and $[RhCl(CO)(PPh_3)_2]$. Our efforts to obtain single crystal of the complex were unsuccessful. Yield: 80%; MP: 215 °C; Anal. calc. for $C_{17}H_{12}N_3O_2RhS$ (%): C, 48.01; H, 2.84; N, 9.88; S, 7.54. Found (%): C, 48.27; H, 2.60; N, 9.63; S, 7.80. IR (KBr, cm^{-1}): 1953 (C≡O); 1627 (quinone C═O); 1584 (C═N); 757 (C–S). UV–Vis (λmax, nm): 421, 392, 318, 272. ^1H NMR (400 MHz, $CDCl_3$, ppm): 8.88 (s, 1H, NH–CH_3); 7.26–8.31 (m, 8H, Ar–H); 3.33 (s, 3H, CH_3). ^{13}C NMR (100 MHz, $CDCl_3$, ppm): 203.61 (C≡O); 180.10 (quinone C═O); 171.08 (C–S); 160.12 (C═N); 127.20, 129.97, 131.41, 132.74, 132.89, 134.21, 134.33, 139.29, 139.93 (Ar–C); 30.32 (CH_3). ESI-Mass (m/z) = 425.4 [M^+].

2.2.3. Synthesis of [Rh(CO)(L_3)] (**3**)

The synthesis of **3** was carried out by the same procedure as described for **1** with HL_3 and $[RhCl(CO)(PPh_3)_2]$. Our efforts to obtain single crystal of the complex were unsuccessful. Yield: 76%; MP: 229 °C; Anal. calc. for $C_{22}H_{14}N_3O_2RhS$ (%): C, 54.22; H, 2.90; N, 8.62; S, 6.58. Found (%): C, 54.13; H, 2.64; N, 8.50; S, 6.74. IR (KBr, cm^{-1}): 1950 (C≡O); 1615 (quinone C═O); 1581 (C═N); 740 (C–S). UV–Vis (λmax, nm): 444, 389, 337, 299. ^1H NMR (400 MHz, $CDCl_3$, ppm): 11.28 (s, 1H, NH–C_6H_5); 7.26–8.49 (m, 13H, Ar–H). ^{13}C NMR (100 MHz, $CDCl_3$, ppm): 202.76 (C≡O); 182.65 (quinone C═O); 170.88 (C–S); 161.12 (C═N); 124.26, 128.72, 130.06, 131.73, 131.80, 133.75, 133.84, 139.62, 139.90 (Ar–C). ESI-Mass (m/z) = 487.2 [M^+].

2.3. Single crystal X-ray diffraction study

Crystal data were collected on an Oxford/Agilent Gemini diffractometer. Structure was solved using the direct methods program SHELXL [40]. All nonsolvent heavy atoms were located using subsequent difference Fourier syntheses. The structure was refined against F^2 with the program SHELXL [41], in which all data collected were used including negative intensities. All nonsolvent heavy atoms were refined anisotropically. All nonsolvent hydrogen atoms were idealized using the standard SHELXL idealization methods.

2.4. Theoretical calculations

The gas phase geometry of complex **1** was fully optimized using density functional theory (DFT) at the B3LYP level using LANL2DZ basis set and employing the Windows versions of Gaussian 09 [42]. At the same level and basis set, calculations of natural electron population, natural charge for each atom and frontier molecular orbitals of the complex have been performed by natural bond orbital (NBO) analysis on the gas phase optimized structure.

2.5. Catalysis

A mixture of catalyst (3 μmol) and ionic liquid (0.10 mmol) in 2 mL of ethanol was stirred for 15 min. To this solution, nitroalkane (3 mmol) and aldehyde (1 mmol) were then added. The reaction mixture was stirred for 8 h at room temperature and then the solvent was evaporated. The product was separated by repetitive washing of the residue with petroleum ether and ethyl acetate (8:2) mixture. After complete washing, the ionic liquid containing catalyst was dried under vacuum and stored in a desiccator for its use in subsequent catalytic runs. The product was then purified by column chromatography to afford the corresponding adduct as the product. The diastereoselectivity and enantiomeric excess of the products were determined by HPLC analysis. The ^1H NMR data of the products were compared with the literature [43].

2.5.1. 1-Phenyl-2-nitro-propan-1-ol

The ee (87%) was determined by chiral HPLC analysis on a Phenomenex Chiralpack column, 95/5 n-hexane/i-PrOH, 1 mL/min,

t_r (*anti*, major) = 13.8 min, t_r (*anti*, minor) = 15.5 min, t_r (*syn*, major) = 18.9 min, t_r (*syn*, minor) = 21.2 min. ^{1}H NMR (300 MHz, $CDCl_3$, ppm): 7.23–7.47 (m, 5H); 5.28 (d, J = 5.8 Hz, 0.67H) (*anti*); 5.04 (d, J = 4.4 Hz, 0.33H) (*syn*); 4.24–4.32 (m, 1H); 2.76 (s, 0.67H) (*anti*); 2.60 (s, 0.33H) (*syn*); 1.49 (d, J = 2.6 Hz, 2.15H) (*anti*); 1.25 (d, J = 3.2 Hz, 0.85H) (*syn*).

2.5.2. 1-(4-Methoxyphenyl)-2-nitro-propan-1-ol

The ee (78%) was determined by chiral HPLC analysis on a Phenomenex Chiralpack column, 90/10 n-hexane/i-PrOH, 1 mL/min, t_r (*anti*, major) = 11.5 min, t_r (*anti*, minor) = 13.2 min, t_r (*syn*, major) = 16.4 min, t_r (*syn*, minor) = 18.7 min. ^{1}H NMR (300 MHz, $CDCl_3$, ppm): 7.44–7.70 (m, 2H); 6.86–7.02 (m, 2H); 5.42 (d, J = 5.8 Hz, 0.69H) (*anti*); 4.92 (d, J = 5.8 Hz, 0.31H) (*syn*); 4.38–4.61 (m, 1H); 3.88 (s, 3H); 2.80 (s, 0.76H) (*anti*); 2.42 (s, 0.24H) (*syn*); 1.58 (d, J = 3.2 Hz, 2.14H) (*anti*); 1.22 (d, J = 3.6 Hz, 0.86H) (*syn*).

2.5.3. 1-(4-Chlorophenyl)-2-nitro-propan-1-ol

The ee (73%) was determined by chiral HPLC analysis on a Phenomenex Chiralpack column, 90/10 n-hexane/i-PrOH, 1 mL/min, t_r (*anti*, major) = 15.2 min, t_r (*anti*, minor) = 16.9 min, t_r (*syn*, major) = 24.0 min, t_r (*syn*, minor) = 21.7 min. ^{1}H NMR (300 MHz, $CDCl_3$, ppm): 7.58–7.76 (m, 2H); 7.18–7.30 (m, 2H); 5.66 (d, J = 5.8 Hz, 0.68H) (*anti*); 5.30 (d, J = 5.0 Hz, 0.32H) (*syn*); 4.68–4.82 (m, 1H); 2.90 (s, 0.71H) (*anti*); 2.64 (s, 0.29H) (*syn*); 1.58 (d, J = 5.8 Hz, 2.18H) (*anti*); 1.20 (d, J = 5.8 Hz, 0.82H) (*syn*).

2.5.4. 1-(4-Nitrophenyl)-2-nitro-propan-1-ol

The ee (92%) was determined by chiral HPLC analysis on a Phenomenex Chiralpack column, 80/20 n-hexane/i-PrOH, 1 mL/min, t_r (*anti*, major) = 16.0 min, t_r (*anti*, minor) = 17.7 min, t_r (*syn*, major) = 20.2 min, t_r (*syn*, minor) = 22.7 min. ^{1}H NMR (300 MHz, $CDCl_3$, ppm): 7.51–7.76 (m, 2H); 6.98–7.14 (m, 2H); 5.26 (d, J = 5.2 Hz, 0.65H) (*anti*); 4.99 (d, J = 5.6 Hz, 0.35H) (*syn*); 4.31–4.52 (m, 1H); 2.94 (s, 0.75H) (*anti*); 2.50 (s, 0.25H) (*syn*); 1.40 (d, J = 2.6 Hz, 2.10H) (*anti*); 1.16 (d, J = 3.2 Hz, 0.90H) (*syn*).

2.5.5. 1-(Naphthalen-1-yl)-2-nitro-propan-1-ol

The ee (83%) was determined by chiral HPLC analysis on a Phenomenex Chiralpack column, 98/2 n-hexane/i-PrOH, 1 mL/min, t_r (*anti*, major) = 30.5 min, t_r (*anti*, minor) = 34.0 min, t_r (*syn*, major) = 46.1 min, t_r (*syn*, minor) = 53.2 min. ^{1}H NMR (300 MHz, $CDCl_3$, ppm): 8.26 (d, J = 5.8 Hz, 1H); 7.68–7.82 (m, 2H); 7.26–7.38 (m, 4H); 5.90 (dd, $J_1 = J_2$ = 2.8 Hz, 1H); 5.14–5.20 (m, 1H); 2.86 (s, 1H); 1.56 (d, J = 5.4 Hz, 2.52H) (*anti*); 1.24 (d, J = 5.6 Hz, 0.48H) (*syn*).

2.5.6. 1-Cyclohexyl-2-nitro-propan-1-ol

The ee (94%) was determined by chiral HPLC analysis on a Phenomenex Chiralpack column, 97/3 n-hexane/i-PrOH, 1 mL/min, t_r (*anti*, major) = 15.7 min, t_r (*anti*, minor) = 19.0 min, t_r (*syn*, major) = 25.3 min, t_r (*syn*, minor) = 17.5 min. ^{1}H NMR (300 MHz, $CDCl_3$, ppm): 4.61–4.72 (m, 1H); 3.97 (d, J = 4.8 Hz, 0.84H) (*anti*); 3.76 (d, J = 4.4 Hz, 0.16H) (*syn*); 2.40 (s, 1H); 1.76–1.88 (m, 1H); 1.40 (d, J = 6.8 Hz, 2.20H) (*anti*); 1.26 (d, J = 5.2 Hz, 0.80H) (*syn*).

2.5.7. 1-Phenyl-2-nitro-butan-1-ol

The ee (81%) was determined by chiral HPLC analysis on a Phenomenex Chiralpack column, 95/5 n-hexane/i-PrOH, 1 mL/min, t_r (*anti*, major) = 26.7 min, t_r (*anti*, minor) = 22.5 min, t_r (*syn*, major) = 31.2 min, t_r (*syn*, minor) = 28.5 min. ^{1}H NMR (300 MHz, $CDCl_3$, ppm): 7.18–7.52 (m, 5H); 5.28 (d, J = 2.8 Hz, 0.83H) (*anti*); 4.98 (d, J = 2.4 Hz, 0.17H) (*syn*); 4.38–4.52 (m, 1H); 2.76 (s, 0.83H) (*anti*); 2.48 (s, 0.17H) (*syn*), 1.48–1.68 (m, 2H); 0.90 (t, J = 2.8 Hz, 2.48H) (*anti*); 0.70 (t, J = 3.2 Hz, 0.52H) (*syn*).

2.5.8. 1-(4-Methoxyphenyl)-2-nitro-butan-1-ol

The ee (93%) was determined by chiral HPLC analysis on a Phenomenex Chiralpack column, 95/5 n-hexane/i-PrOH, 1 mL/min, t_r (*anti*, major) = 20.2 min, t_r (*anti*, minor) = 21.3 min, t_r (*syn*, major) = 28.6 min, t_r (*syn*, minor) = 31.0 min. ^{1}H NMR (300 MHz, $CDCl_3$, ppm): 7.20–7.24 (m, 5H); 5.16 (d, J = 2.6 Hz, 0.86H) (*anti*); 4.88 (d, J = 2.6 Hz, 0.14H) (*syn*); 4.49–4.67 (m, 1H); 3.84 (s, 3H); 3.03 (s, 0.86H) (*anti*); 2.90 (s, 0.14H) (*syn*); 2.10–2.28 (m, 2H); 1.07 (t, J = 3.4 Hz, 2.54H) (*anti*); 0.96 (t, J = 4.2 Hz, 0.46H) (*syn*).

2.5.9. 1-(4-Chlorophenyl)-2-nitro-butan-1-ol

The ee (81%) was determined by chiral HPLC analysis on a Phenomenex Chiralpack column, 95/5 n-hexane/i-PrOH, 1 mL/min, t_r (*anti*, major) = 12.3 min, t_r (*anti*, minor) = 13.8 min, t_r (*syn*, major) = 21.5 min, t_r (*syn*, minor) = 17.7 min. ^{1}H NMR (300 MHz, $CDCl_3$, ppm): 7.18–7.30 (m, 5H); 5.14 (d, J = 2.8 Hz, 0.79H) (*anti*); 4.96 (d, J = 2.4 Hz, 0.21H) (*syn*); 4.44–4.54 (m, 1H); 3.08 (s, 0.79H) (*anti*); 2.72 (s, 0.21H) (*syn*); 1.68–2.02 (m, 2H); 1.02 (t, J = 3.2 Hz, 3H).

2.5.10. 1-Cyclohexyl-2-nitro-butan-1-ol

The ee (84%) was determined by chiral HPLC analysis on a Phenomenex Chiralpack column, 99/1 n-hexane/i-PrOH, 1 mL/min, t_r (*anti*, major) = 44.3 min, t_r (*anti*, minor) = 48.2 min, t_r (*syn*, major) = 60.0 min, t_r (*syn*, minor) = 56.4 min. ^{1}H NMR (300 MHz, $CDCl_3$, ppm): 4.48–4.70 (m, 1H); 3.76 (d, J = 4.2 Hz, 0.91H) (*anti*); 3.60 (d, J = 4.6 Hz, 0.09H) (*syn*); 2.34 (s, 1H); 1.80–2.11 (m, 2H); 1.26–1.50 (m, 11H); 0.95 (t, J = 4.8 Hz, 3H).

3. Results and discussion

The synthetic route of rhodium(I) complexes was shown in Scheme 1. The isolated complexes were stable at room temperature, non-hygroscopic in nature and highly soluble in common organic solvents such as dichloromethane, chloroform, benzene, acetonitrile, ethanol, methanol, dimethylformamide and dimethylsulfoxide. All the complexes were structurally characterized by elemental analyses, IR, electronic, NMR and ESI-Mass spectra. For further confirmation, the structure of complex **1** was elucidated by X-ray crystallographic analysis.

3.1. Spectroscopic studies

The IR spectra of the ligands and the corresponding rhodium(I) complexes provided significant information about the metal-ligand bonding. A strong vibration appeared at 1596–1598 and 1630–1634 cm^{-1} in the ligands corresponding to azomethine ν(C=N) and quinone carbonyl ν(C=O) shifted to lower wave numbers 1578–1584 and 1615–1627 cm^{-1} in all the complexes indicating the participation of azomethine nitrogen and quinone oxygen in bonding [44] with rhodium atom. A sharp band was observed at 807–843 cm^{-1}, ascribed to ν(C=S) in the ligands, has completely

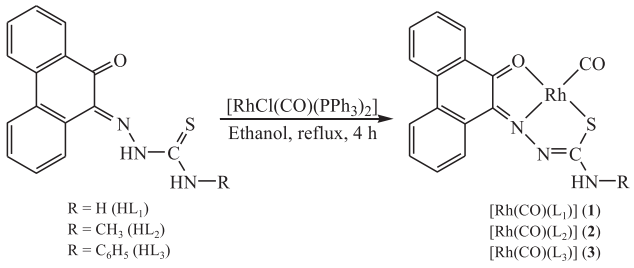

Scheme 1. Synthetic route of rhodium(I) complexes.

disappeared in the spectra of all the new rhodium complexes and the appearance of a new band at 740–757 cm^{-1} due to ν(C–S) indicate the coordination of the sulfur atom after enolization followed by deprotonation [45]. Further, the hydrazinic ν(N–H) band appeared at 3111–3148 cm^{-1} in the free ligands disappeared in the complexes, suggesting deprotonation of the –NH group [46]. All the complexes displayed a medium to strong band in the region 1950–1953 cm^{-1}, which was attributed to the terminally coordinated carbonyl group, ν(C≡O) [47]. Electronic spectra of the complexes showed two very intense absorptions in the UV region together with two intense absorptions in the visible region. The absorptions in the UV region were assignable to transitions within the ligand orbitals while those in the visible region were probably due to metal-to-ligand charge-transfer transitions.

In the ^{1}H NMR spectra, singlet that appeared for the hydrazinic ν(N–H) proton of the free ligands at 14.41–14.81 ppm was absent in the complexes, supporting the enolization and coordination of the thiolate sulfur to the rhodium(I) ion. The terminal NH_2 protons in ligands HL_1 were magnetically non-equivalent, have shown two singlets at 9.07 and 9.36 ppm. These protons became equivalent upon formation of rhodium complexes and appeared as a singlet at 9.41 ppm. Ligands HL_2, HL_3 and their corresponding complexes showed singlet in the region 8.35–11.28 ppm was assigned to NH methyl and NH phenyl protons. In the spectra of all the complexes, the multiplet appeared around 7.26–8.49 ppm was assigned to aromatic protons of ligands. Further, the methyl protons appeared in the region 2.98–3.33 ppm. The ^{13}C NMR spectra of the complexes showed a peak at 202.76–203.87 ppm region was due to terminal C≡O carbon. The presence of peak at 180.24–182.65 ppm region was assigned to quinone carbonyl (C═O) carbon. The azomethine (C═N) carbon exhibited a peak in the region of 159.96–161.12 ppm. In addition, the presence of peak in the region 170.88–171.82 ppm was assigned to thiosemicarbazone C–S carbon. The appearance of sharp singlet at 30.32 ppm was assigned to methyl carbon. The aromatic carbons appeared in the region of 124.26–139.93 ppm. The *m*/*z* value of the molecular ion peak for the complexes **1**–**3** was obtained at 411.4, 425.4 and 487.2 [M^+] respectively. The calculated molecular mass correspond to these complexes was 411.2, 425.2 and 487.3. The obtained molecular masses were in good agreement with that of the calculated molecular masses.

3.2. X-ray crystallography

Single crystals of **1** were obtained from slow evaporation of a mixture of chloroform and ethanol at room temperature. A red crystal of approximate dimensions 0.32 × 0.25 × 0.16 mm was isolated and the single crystal X-ray diffraction experiment was carried out at 293 K. From the unit cell dimensions, it was clear that the crystal was monoclinic belonging to the $P2_1/c$ space group. Ellipsoidal plot of complex **1** labeled with atom numbering scheme was shown in Fig. 1. Crystallographic data was given in Table 1. The coordination geometry around the rhodium(I) ion was slightly distorted square planar, where the basal plane was constructed of quinone oxygen, the imine nitrogen and the thiolate sulfur atom of the ligand in its mononegative tridentate ONS fashion and carbonyl. The imine nitrogen atom was *trans* to the carbonyl group and the quinone oxygen was *trans* to the thiolate sulfur atom. The bond lengths were 1.940(18) [Rh(1)–N(1)], 2.163(13) [Rh(1)–O(1)], 2.339(6) [Rh(1)–S(1)] and 2.281(6) Å [Rh(1)–C(16)]. Comparison of the bond lengths in the coordinated thiosemicarbazone ligand with those in the uncoordinated ligand [14d] shows that upon coordination the C–S bond has undergone elongation, whereas the adjacent C–N bond has undergone contraction. These changes in bond lengths were consistent with the deprotonation of ligand upon complexation. The tridentate ONS ligand coordinated

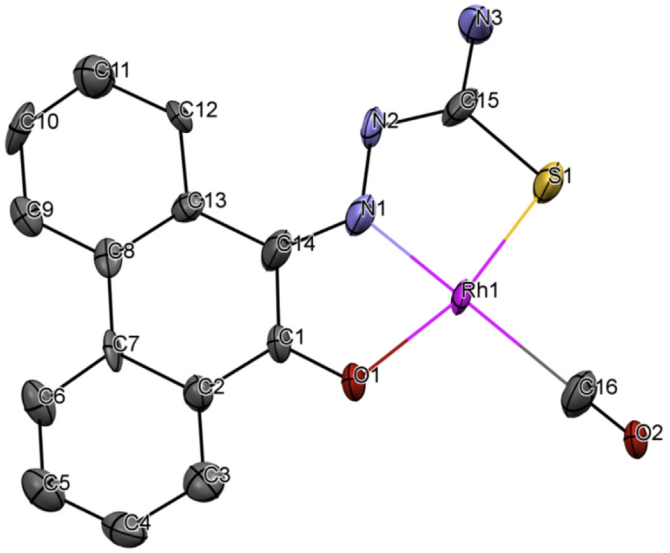

Fig. 1. ORTEP view of complex **1**. Thermal ellipsoids were drawn at 30% probability level. The hydrogen atoms were omitted for clarity.

Table 1
Crystal data and structure refinement parameters of the complex **1**.

	1
Empirical formula	$C_{16}H_{10}N_3RhO_2S$
Formula weight	411.24
Crystal dimensions (mm^3)	0.32 × 0.25 × 0.16
Temperature (K)	293(2)
Wavelength (Å)	0.71073
Crystal system	Monoclinic
Space group	P21/c
Unit cell dimensions (Å, °)	a = 10.6153(6) b = 5.1839(16) c = 35.6301(9)
Volume ($Å^3$)	1960.4(6)
Z	4
Calculated density (Mg/m^3)	1.393
Absorption coefficient (mm^{-1})	0.987
F(000)	816.0
Theta range for data collection (°)	2.32 to 30.65
Absorption correction	Multi-scan
Refinement method	Full-matrix least-squares on F^2
Data/restraints/parameters	6066/0/326
Goodness-of-fit on F^2	1.032
R indices [$I > 2\sigma(I)$]	$R1$ = 0.1006, $wR2$ = 0.2089
R indices (all data)	$R1$ = 0.1465, $wR2$ = 0.2268

equatorially to the metal ion with the formation of two five membered ring with the bite angles of 83.7(6)° [N(1)–Rh(1)–O(1)] and 82.7(6)° [N(1)–Rh(1)–S(1)] were less than 90° while the angles of 96.0(3)° [O(1)–Rh(1)–C(16)] and 97.6(2)° [S(1)–Rh(1)–C(16)] were greater than 90°. This results showed significant distortion of the {RhONS(CO)} core from the ideal square planar geometry.

3.3. Computational

3.3.1. Geometry optimization

A DFT calculation was performed on the complex **1**. The geometry was optimized without symmetry constraints. The structural parameters (distances and angles) of optimized geometry (Table 2) obtained by DFT/B3LYP method have a good agreement with X-ray

structural data. The negligible difference between experimental and theoretical data refers to the fact that the experimental data belong to the solid state and the lattice with interactions in the crystal structure, while the calculated values refer to a single molecule in the gas phase.

3.3.2. Frontier molecular orbitals

The electronic, optical properties and chemical reactions of the complexes mainly depend on frontier molecular orbitals [48]. Hence, the composition and energy levels of the HOMO and LUMO orbitals may provide insight into the chemical behavior of such species and those of **1** were depicted in Fig. 2. Positive and negative regions were shown in red and green colors, respectively. Fig. 2 illustrate that the highest occupied molecular orbital was mainly delocalized on metal with some contributions from ligands and the lowest unoccupied molecular orbital was mainly delocalized on ligands with minor contributions from metal. Since the first electron transfer occurs from the highest occupied molecular orbital (HOMO) to lowest unoccupied molecular orbital (LUMO), it can be inferred that the first electron transfer in **1** was related to MLCT.

3.3.3. Natural bond order analysis (NBO)

The calculated atomic charge and electron configuration of donor atoms and metal center were listed in Table 3. The calculated formal charge on the central ion was quite smaller as compared to the formal oxidation state of the metal (+1). The charges on the carbon and nitrogen atoms were positive, whereas the oxygen and sulfur atoms were negatively charged. In a similar way, the calculated electronic configurations of the donor atoms with reference to s and p orbitals were less than the expected values of valance orbitals, while the computed electron population in central ion was more than the expected value for Rh^{I} with d^{8} electron configuration. This confirms the electron transmission of donor atoms towards the central metal.

3.3.4. Catalytic nitroaldol (Henry) reaction

In order to find optimal reaction conditions, the influence of time, solvent and the catalyst concentration on the yield were investigated. Our initial studies on the development of new rhodium(I) complexes in ionic liquid for nitroaldol condensation were carried out with benzaldehyde and nitroethane as model substrates using complex **1** as catalyst. The first set reactions were run with constant concentration of catalyst (2.0 μmol) at various time intervals in different solvents. The best conversion was observed in ethanol and the least conversion was observed in toluene at 8 h (Fig. 3). Next, we focused the effect of catalyst concentration on the catalyst activity. The catalyst amount was varied from 0.5 to 4.0 μmol in ethanol under similar reaction conditions. When the catalyst amount was 3.0 μmol, an excellent yield was obtained. It

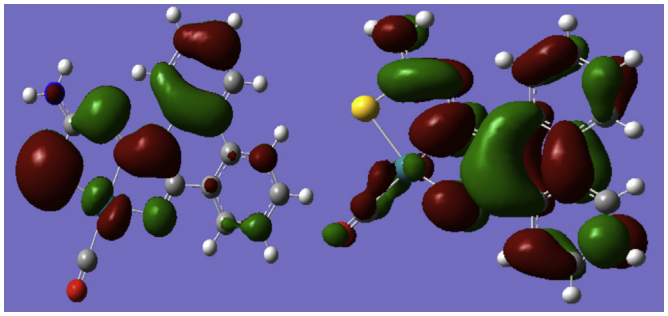

Fig. 2. Calculated HOMO and LUMO for **1**.

Table 3
Charge (a.u.) and electron configuration of the complex **1**.

Atom	Charge	Electronic configuration
Rh	−0.495498	[core]5s(0.45)4d(8.34)
O	−0.430828	[core]2s(1.68)2p(4.86)
N	0.792792	[core]2s(1.32)2p(3.87)
S	−0.382028	[core]3s(1.74)3p(4.32)
C	1.376631	[core]2s(1.23)2p(2.07)

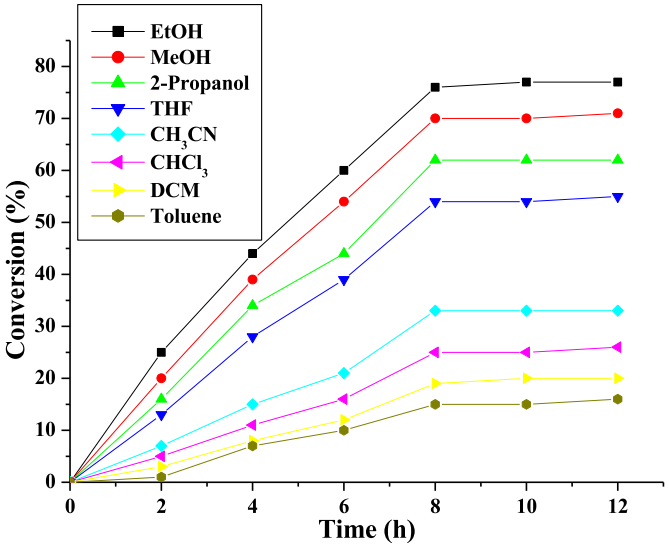

Fig. 3. Optimization of solvent for catalytic nitroaldol reaction. Reaction conditions: Benzaldehyde (1 mmol), nitroethane (3 mmol), catalyst (2 μmol) and ionic liquid (0.1 mmol) was stirred at r.t for 8 h.

Table 2
Selective experimental (X-ray) and calculated (DFT) bond distances (Å) and bond angles (°) of the complex **1**.

	Interatomic distances (Å)			Bond angles (°)	
	Experimental	Calculated		Experimental	Calculated
Rh–N(1)	1.940(18)	2.0536	N(1)–Rh–O(1)	83.7(6)	78.393
Rh–O(1)	2.163(13)	2.0802	N(1)–Rh–S(1)	82.7(6)	84.332
Rh–S(1)	2.339(6)	2.4054	O(1)–Rh–C(16)	96.0(3)	99.444
Rh–C(16)	2.281(6)	1.8905	S(1)–Rh–C(16)	97.6(2)	97.410
C(15)–N(2)	1.35(3)	1.3453	C(15)–S(1)–Rh	97.6(8)	91.925
C(15)–N(3)	1.35(3)	1.3421	N(2)–N(1)–Rh	123.7(16)	122.546
			C(1)–O(1)–Rh	109.0(12)	112.870
			C(14)–N(1)–Rh	112.5(13)	116.641
			N(2)–C(15)–N(3)	116.6(17)	115.838
			O(1)–Rh–S(1)	166.4(3)	162.639
			N(1)–Rh–C(16)	179.7(6)	171.611

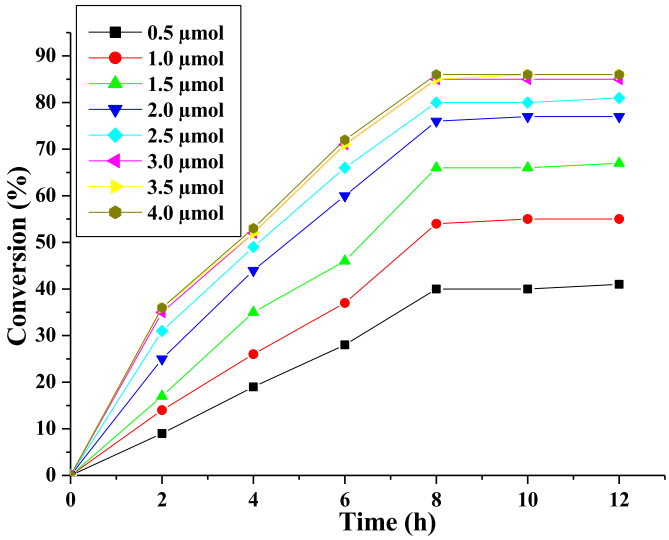

Fig. 4. Optimization of catalyst loading in nitroaldol reaction. Reaction conditions: Benzaldehyde (1 mmol), nitroethane (3 mmol) and ionic liquid (0.1 mmol) in ethanol was stirred at r.t for 8 h.

was also observed that moderate yield was obtained even at very low catalyst loading of 1.0 µmol (Fig. 4). It was noteworthy that the reaction not able to proceed without a catalyst under similar reaction conditions. In order to choose the best catalyst among the synthesized complexes, the nitroaldol reaction of benzaldehyde with nitroethane was carried out using the catalysts **1**, **2** and **3** under the above optimized conditions. From the results, the complex **2** was found to the best catalyst and showed the yield of 94% (Fig. 5). The order of reactivity of complexes with respect to different substitutions on thiosemicarbazone fragment of the ligands was given by, **2** > **1** > **3**.

The above optimized reaction protocol for nitroaldol reaction was further extended to various aromatic aldehydes using the complex **2** as catalyst in presence of [emim]BF_4 as ionic liquid and the results were summarized in Table 4. When nitroethane was used, all the aldehydes used in the present study showed only marginal difference

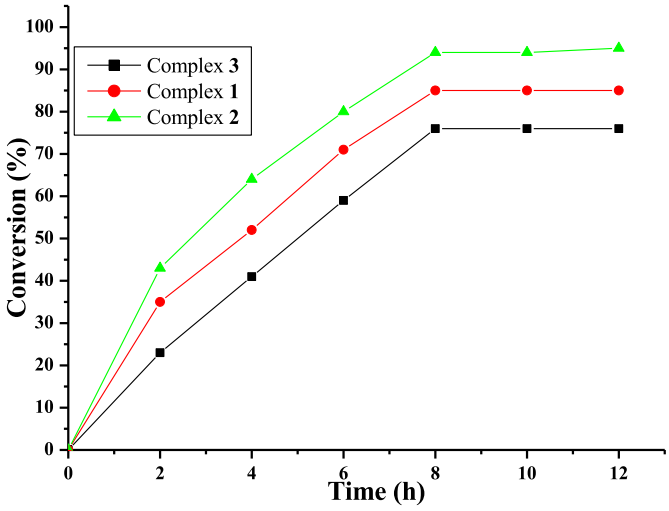

Fig. 5. Selection of suitable catalyst for catalytic nitroaldol reaction. Reaction conditions: Benzaldehyde (1 mmol), nitroethane (3 mmol), catalyst (3 µmol) and ionic liquid (0.1 mmol) in ethanol was stirred at r.t for 8 h.

in the yield of the products irrespective of the electron withdrawing or electron donating substituents on the phenyl ring of aldehyde. The products were mixtures of the β-nitroalkanol diastereoisomers (*anti* and *syn* forms) with overall conversions upto 97% and predominance of the anti isomer (*anti*/*syn* selectivity = 89.6:10.4) (entries 1–4). The substrates 1-naphthaldehyde and cyclohexane carboxaldehyde react with nitroethane exhibited good yields with high diastereoselectivity (entries 5 and 6). However, among all the substrate used here, the best result in term of activity and diastereoselectivity was achieved with 4-nitro benzaldehyde (entry 4). Because of the good results obtained with the addition of nitroethane to aldehydes, we decided to extend the reaction to nitropropane. Diastereoselectivity was dramatically improved when 1-nitropropane was used and affords the desired product in good to high yields, accompanied by the predominant *anti* diastereomer. Among the substrates, the unsubstituted benzaldehyde gave higher yield when compared to that of electron donating/withdrawing substituent on benzaldehyde (entries 7–9). The substrate cyclohexane carboxaldehyde react with nitropropane exhibited good yield with high diastereoselectivity (enty 10).

Recovery and reusability of catalysts was an important theme in catalysis. This makes the catalysts to be used in many catalytic cycles, there by more commercial for industrial catalysis. The catalyst was recovered and recycled as follows. After completion of the catalytic reaction, the solvent was completely evaporated under reduced pressure and the products were extracted with petroleum ether and ethyl acetate mixture (80:20). The extract was concentrated and purified by column chromatography. The recovered ionic liquid containing the catalyst **2** was dried in vacuum and was used for the subsequent catalytic runs without any further processing. The recovered catalyst worked well up to five catalytic runs with marginal loss in yield. During the catalytic recycle reactions the diastereoselectivity of the product was retained (Table 5). In addition, the present catalytic system works at mild reaction conditions with low reaction time, low catalyst loading and the efficiency in terms of the yield of products was higher than the existing catalytic systems [36,37,49–52].

A proposed mechanism for nitroaldol reaction of benzaldehyde with nitroethane in presence of rhodium complex **1** has been shown in Scheme 2. The aldehyde was coordinated to the vacant d orbital of the rhodium through the lone pair of the oxygen forming a penta-coordinate transition state (**I**) thereby increasing the electrophilicity of the carbonyl group. The coordination number of the rhodium center may be extended to six from five on further addition of active nucleophile, nitronate ion forming transition state (**II**) where the nitronate ion attacks the activated aldehyde to give the nitroaldol product. With respect to the stereo chemistry, the attachment through the hydrogen side is more favorable compared to that of highly steric phenyl group side. Hence, *anti* attachment predominantly takes place and form *anti* product as a major one. In order to confirm the intermediates formed during the course of reaction, the ESI-Mass spectrum was recorded for the reaction of benzaldehyde with nitroethane in presence of the complex **1**. It was observed that gradual replacement of main peak associated with the complex **1**, (m/z = 411) by new peaks assigned to ([Rh(CO)(L_1)(benzaldehyde)]$^+$) (**I**) (m/z = 517) and [Rh(CO)(L_1)(benzaldehyde) (nitroethane)]$^+$) (**II**) (m/z = 591). These peak displacements support the coordination of substrates with metal and forming two intermediates.

4. Conclusion

In this study, new four coordinated rhodium(I) complexes containing 9,10-phenanthrenequinone appended with thiosemicarbazone derivatives have been synthesized and characterized. The molecular structure of a representative complex **1**, was

Table 4
Nitroaldol (Henry) reaction of nitroethane and nitropropane with various aldehydes.[a]

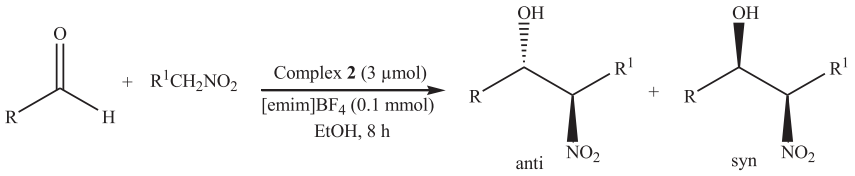

Entry	R	R^1	Yield (%)[a]	*anti*:*syn* (%)[b]	ee of *anti* (%)[b]
1	Ph	Me	94	68.8:31.2	87
2	4-MeO–C_6H_4	Me	96	75.0:25.0	78
3	4-Cl–C_6H_4	Me	94	63.8:36.2	73
4	4-NO_2–C_6H_4	Me	97	89.6:10.4	92
5	1-Naphthyl	Me	91	71.3:28.7	83
6	Cyclohexyl	Me	88	86.5:13.5	94
7	Ph	Et	98	95.6:4.4	81
8	4-MeO–C_6H_4	Et	97	72.4:27.6	93
9	4-Cl–C_6H_4	Et	90	77.2:22.8	81
10	Cyclohexyl	Et	92	90.7:9.3	84

[a] Determined by column chromatography.
[b] Determined by chiral HPLC analysis.

Table 5
Recyclability test of the catalyst **2** using benzaldehyde and nitroethane as model substrates in presence of ionic liquid [emim]BF_4.

Run	Yield (%)[a]	*anti*:*syn* (%)[b]	ee of *anti* (%)[b]
1st	94	68.8:31.2	87
2nd	94	68.8:31.2	87
3rd	93	68.8:31.2	87
4th	92	68.8:31.2	87
5th	91	68.8:31.2	87

[a] Determined by column chromatography.
[b] Determined by chiral HPLC analysis.

determined by single crystal X-ray diffraction method and reveals a distorted square planar geometry around the rhodium(I) ion. To support the solid state structure, the geometric parameter of **1** was calculated using the density functional theory at B3LYP level with LANL2DZ basis set and compared with the experimental data.

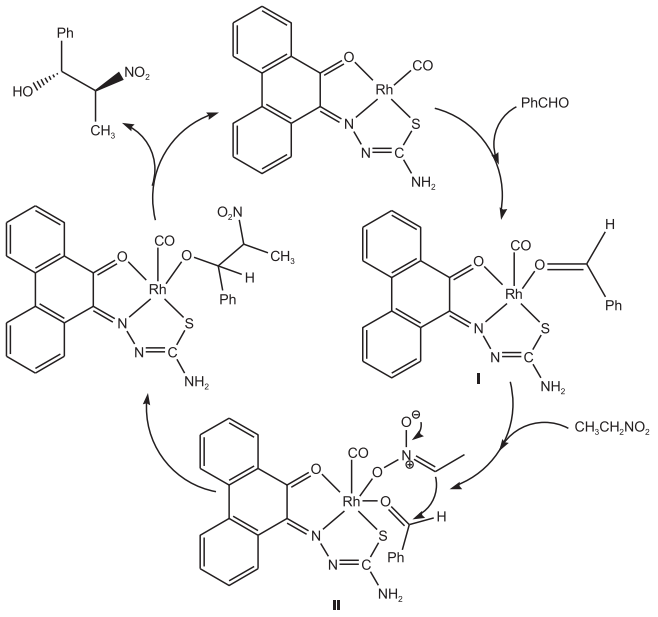

Scheme 2. Possible mechanistic pathway for rhodium(I) catalyzed nitroaldol reaction.

Catalytic results showed that the synthesized rhodium(I) complexes were effective catalysts for the diastereoselective nitroaldol reaction, leading to β-nitroalkanols with high yield and predominance of the *anti* diastereoisomer. The present ionic liquid mediated nitroaldol protocol was recyclable (up to five cycles) with no significant loss in its performance. Optimized catalyst **2**, promotes the diastereoselective Henry reaction between various aromatic aldehyde and nitroalkane substrates and gives the corresponding *anti*-selective adduct with up to 98% yield and 95.6:4.4 *anti*/*syn* selectivity. A possible catalytic mechanism was also suggested for the asymmetric Henry reactions. Moreover, in comparison with other reported metal catalysts for the Henry reaction, our catalytic system seems to be the best with respect to activity, catalyst loading, time and recyclability.

Acknowledgment

The authors express their sincere thanks to Council of Scientific and Industrial Research (CSIR), New Delhi, India [Grant No. 01(2437)/10/EMR-II] for financial support. One of the authors (PA) thanks CSIR for the award of Senior Research Fellowship. The authors wish to record grateful thanks to Dr. V. Jayamani, Department of Chemistry, Sri Sarada College for Women, Salem-636016, Tamil Nadu, India for discussion in DFT studies.

Supplementary material

CCDC 1035060 contains the supplementary crystallographic data for the complex **1**. These data can be obtained free of charge via www.ccdc.cam.ac.uk/data request/cif.

References

[1] P.G. Cozzi, Chem. Soc. Rev. 33 (2004) 410.
[2] R. Drozdzak, B. Allaert, N. Ledoux, I. Dragutan, V. Dragutan, F. Verpoort, Coord. Chem. Rev. 249 (2005) 3055.
[3] T. Katsuki, Chem. Soc. Rev. 33 (2004) 437.
[4] C.M. Che, J.S. Huang, Coord. Chem. Rev. 242 (2003) 97.
[5] K.C. Gupta, A.K. Sutar, Coord. Chem. Rev. 252 (2008) 1420.
[6] A.G. Quiroga, C.N. Ranninger, Coord. Chem. Rev. 248 (2004) 119.
[7] T.S. Lobana, R. Sharma, G. Bawa, S. Khanna, Coord. Chem. Rev. 253 (2009) 977.
[8] J.S. Casas, M.D. Couce, J. Sordo, Coord. Chem. Rev. 256 (2012) 3036.
[9] M.J.M. Campbell, Coord. Chem. Rev. 15 (1975) 279.
[10] S. Padhye, G.B. Kauffman, Coord. Chem. Rev. 63 (1985) 127.

[11] J.S. Casas, M.S. Garcia-Tasende, J. Sordo, Coord. Chem. Rev. 209 (2000) 197.
[12] R.B. Singh, B.S. Garg, R.P. Singh, Talanta 25 (1978) 619.
[13] (a) M. Muthukumar, S. Sivakumar, P. Viswanathamurthi, R. Karvembu, R. Prabhakaran, K. Natarajan, J. Coord. Chem. 63 (2010) 296;
(b) R. Manikandan, P. Viswnathamurthi, Spectrochim. Acta A 97 (2012) 864;
(c) M. Nirmala, R. Manikandan, G. Prakash, P. Viswanathamurthi, Appl. Organometal. Chem. 28 (2014) 18;
(d) R. Manikandan, P. Vijayan, P. Anitha, G. Prakash, P. Viswanathamurthi, R.J. Butcher, K. Velmurugan, R. Nandhakumar, Inorg. Chim. Acta 421 (2014) 80;
(e) R. Manikandan, P. Anitha, G. Prakash, P. Vijayan, P. Viswanathamurthi, Polyhedron 81 (2014) 619;
(f) R. Manikandan, N. Chitrapriya, Y.J. Jang, P. Viswanathamurthi, RSC Adv. 3 (2013) 11647;
(g) S. Selvamurugan, R. Ramachandran, P. Viswanathamurthi, Biometals 26 (2013) 741;
(h) P. Vijayan, P. Viswanathamurthi, V. Silambarasan, D. Velmurugan, K. Velmurugan, R. Nandhakumar, R.J. Butcher, T. Silambarasan, R. Dhandapani, J. Organomet. Chem. 768 (2014) 163;
(i) G. Prakash, R. Manikandan, P. Viswanathamurthi, K. Velmurugan, R. Nandhakumar, J. Photochem. Photobiol. B 138 (2014) 63;
(j) R. Ramachandran, G. Prakash, S. Selvamurugan, P. Viswanathamurthi, J.G. Malecki, V. Ramkumar, Dalton Trans. 43 (2014) 7889;
(k) S. Selvamurugan, P. Viswanathamurthi, A. Endo, T. Hashimoto, K. Natarajan, J. Coord. Chem. 66 (2013) 4052;
(l) R. Manikandan, P. Viswanathamurthi, K. Velmurugan, R. Nandhakumar, T. Hashimoto, A. Endo, J. Photochem. Photobiol. B 130 (2014) 205.
[14] (a) P. Anitha, R. Manikandan, A. Endo, T. Hashimoto, P. Viswanathamurthi, Spectrochim. Acta A 99 (2012) 174;
(b) P. Anitha, N. Chitrapriya, Y.J. Jang, P. Viswanathamurthi, J. Photochem. Photobiol. B 129 (2013) 17;
(c) P. Anitha, P. Viswanathamurthi, B. Misini, W. Linert, Monatsh. Chem. 144 (2013) 1787;
(d) P. Anitha, P. Viswanathamurthi, D. Kesavan, R.J. Butcher, J. Coord. Chem. 68 (2015) 321.
[15] W.A. Herrmann, B. Cornils, Applied Homogeneous Catalysis with Organometallic Compounds, VCH Weinheim, 1999.
[16] G.W. Parshall, S.D. Ittel (Eds.), Homogeneous Catalysis, second ed., Wiley-Interscience, New York, 1992, p. 96.
[17] K. Weissermel, H.J. Arpe (Eds.), Industrial Organic Chemistry, third ed., VCH, Weinheim, 1997.
[18] H.M. Colquhoun, D.J. Thompson, M.V. Twigg, Carbonylation: Direct Synthesis of Carbonyl Compounds, Plenum Press, New York (, 1991.
[19] A. Haynes, P.M. Maitlis, G.E. Morris, G.J. Sunley, H. Adams, P.W. Badger, C.M. Bowers, B. Cook, P.I.P. Elliot, T. Ghaffar, H. Green, T.R. Griffin, M. Payne, J.-M. Pearson, M.J. Taylor, P.W. Vickers, R.J. Watt, J. Am. Chem. Soc. 126 (2004) 2847.
[20] T.W. Dekleva, D. Foster, Adv. Catal. 34 (1986) 81.
[21] H. Kidwell, January 2008, www.in-pharmatechnologist.com/content/ (accessed 16.03.10).
[22] D.K. Seth, S. Bhattacharya, J. Org. Chem. 696 (2011) 3779.
[23] N.F. Stuurman, A. Muller, J. Conradie, Trans. Met. Chem. 38 (2013) 429.
[24] (a) G. Rosini, in: B.M. Trost, I. Fleming (Eds.), Comprehensive Organic Synthesis 2, Pergamon, Oxford, UK, 1999, p. 321;
(b) H.W. Pinnick, in: L.A. Paquette (Ed.), Organic Reactions, vol. 38, Wiley, New York, 1990 (Chapter 3).
[25] (a) G. Rosini, B.M. Trost, Eds., vol. 2, Pergamon, New York, 1991, 321. (b) K. Iseki, S. Oishi, H. Sasai, M. Shibasaki, Tetrahedron Lett. 37 (1996) 9081;
(c) A. Barco, S. Benetti, C. Risi, G. Polloni, Tetrahedron Lett. 37 (1996) 7599;
(d) H. Sasai, M. Hiroi, Y. Yamada, M. Shibasaki, Tetrahedron Lett. 38 (1997) 6031;
(e) M. Shibasaki, H. Sasai, T. Arai, Angew. Chem. Int. Ed. Engl. 36 (1997) 1236.
[26] W. Jin, X. Li, Y. Huang, F. Wu, B. Wan, Chem. Eur. J. 16 (2010) 8259.
[27] N. Gogoi, J. Boruwa, N.C. Barua, Tetrahedron Lett. 46 (2005) 7581.
[28] G. Blay, V. Hernández-Olmos, J.R. Pedro, Tetrahedron Asymm. 21 (2010) 578.
[29] Z. Guo, Y. Deng, S. Zhong, G. Lu, Tetrahedron Asymm. 22 (2011) 1395.
[30] (a) H. Sasai, T. Suzuki, S. Arai, T. Arai, M. Shibasaki, J. Am. Chem. Soc. 114 (1992) 4418;
(b) M. Shibasaki, N. Yoshikawa, Chem. Rev. 102 (2002) 2187.
[31] (a) T. Arai, R. Takashita, Y. Endo, M. Watanabe, A. Yanagisawa, J. Org. Chem. 73 (2008) 4903;
(b) M. Steurer, C. Bolm, J. Org. Chem. 75 (2010) 3301;
(c) Y. Qiong, G. Qi, Z.M.A. Judeh, Eur. J. Org. Chem. (2011) 4892;
(d) Y. Qiong, G. Qi, Z.M.A. Judeh, Tetrahedron Asymm. 22 (2011) 2065;
(e) F. Liu, S. Gou, L. Li, P. Yan, C. Zhao, J. Mol. Catal. A 379 (2013) 163;
(f) A. Das, R.I. Kureshy, P.S. Subramanian, N.H. Khan, S.H.R. Abdi, H.C. Bajaj, Catal. Sci. Technol. 4 (2014) 411.
[32] (a) B.M. Trost, V.S.C. Yeh, Angew. Chem. Int. Ed. 41 (2002) 861;
(b) B.M. Trost, V.S.C. Yeh, H. Ito, N. Bremeyer, Org. Lett. 4 (2002) 2621;
(c) C. Palomo, M. Oiarbide, A. Laso, Angew. Chem. Int. Ed. 44 (2005) 3881;
(d) A. Bulut, A. Aslan, O.Z. Dogan, J. Org. Chem. 73 (2008) 7373;
(e) H.Y. Kim, K. Oh, Org. Lett. 11 (2009) 5682.
[33] (a) Y. Kogami, T. Nakajima, T. Ikeno, T. Yamada, Synthesis (2004) 1947;
(b) J. Park, K. Lang, K.A. Abboud, S. Hong, J. Am. Chem. Soc. 130 (2008) 16484.
[34] (a) A.S. Zulauf, M. Mellah, E. Schulz, J. Org. Chem. 74 (2009) 2242;
(b) R. Kowalczyk, P. Kwiatkowski, J. Skarzewski, J. Jurczak, J. Org. Chem. 74 (2009) 753.
[35] S. Handa, K. Nagawa, Y. Sohtome, S. Matsunaga, M. Shibasaki, Angew. Chem. Int. Ed. 47 (2008) 3230.
[36] S. Kiyooka, T. Tsutsui, H. Maeda, Y. Kanelo, K. Isobe, Tetrahedron Lett. 36 (1995) 6531.
[37] C. Pettinari, F. Marchetti, A. Cerquetella, R. Pettinari, M. Monari, T.C.O. Mac Leod, L.M.D.R.S. Martins, A.J.L. Pombeiro, Organometallics 30 (2011) 1616.
[38] (a) T. Arai, Y.M.A. Yamada, N. Yamamoto, H. Sasai, M. Shibasaki, Chem. Eur. J. 2 (1996) 1368;
(b) H. Sasai, T. Tokunaga, S. Watanabe, T. Suzuki, N. Itoh, M. Shibasaki, J. Org. Chem. 60 (1995) 7388.
[39] D. Evans, J.A. Osborn, G. Wilkinson, Inorg. Synth. 28 (1990) 79.
[40] G.M. Sheldrick, Acta Crystallogr. Sect. A 46 (1990) 467.
[41] G.M. Sheldrick, SHELXL-97: FORTRAN Program for Crystal Structure Refinement, Gottingen University, 1997.
[42] M.J. Frisch, G.W. Trucks, H.B. Schlegel, G.E. Scuseria, M.A. Robb, J.R. Cheeseman, G. Scalmani, V. Barone, B. Mennucci, G.A. Petersson, H. Nakatsuji, M. Caricato, X. Li, H.P. Hratchian, A.F. Izmaylov, J. Bloino, G. Zheng, J.L. Sonnenberg, M. Hada, M. Ehara, K. Toyota, R. Fukuda, J. Hasegawa, M. Ishida, T. Nakajima, Y. Honda, O. Kitao, H. Nakai, T. Vreven, J.A. Montgomery Jr., J.E. Peralta, F. Ogliaro, M. Bearpark, J.J. Heyd, E. Brothers, K.N. Kudin, V.N. Staroverov, R. Kobayashi, J. Normand, K. Raghavachari, A. Rendell, J.C. Burant, S.S. Iyengar, J. Tomasi, M. Cossi, N. Rega, J.M. Millam, M. Klene, J.E. Knox, J.B. Cross, V. Bakken, C. Adamo, J. Jaramillo, R. Gomperts, R.E. Stratmann, O. Yazyev, A.J. Austin, R. Cammi, C. Pomelli, J.W. Ochterski, R.L. Martin, K. Morokuma, V.G. Zakrzewski, G.A. Voth, P. Salvador, J.J. Dannenberg, S. Dapprich, A.D. Daniels, O. Farkas, J.B. Foresman, J.V. Ortiz, J. Cioslowski, D.J. Fox, Gaussian 09, Revision A.02, Gaussian, Inc., Wallingford CT, 2009.
[43] (a) G. Blay, L.R. Domingo, V. Hernandez-Olmos, J.R. Pedro, Chem. Eur. J. 14 (2008) 4725–4730;
(b) T. Arai, R. Takashita, Y. Endo, M. Watanabe, A. Yanagisawa, J. Org. Chem. 73 (2008) 4903;
(c) T. Arai, M. Watanabe, A. Yanagisaka, Org. Lett. 9 (2007) 3595.
[44] A. Castineiras, R. Pedrido, Dalton Trans. 39 (2010) 3572.
[45] P. Kalaivani, R. Prabhakaran, P. Poornima, F. Dallemer, K. Vijayalakshmi, V. Vijaya Padma, K. Natarajan, Organometallics 31 (2012) 8323.
[46] M. Mohan, N.S. Gupta, M. Kumar, Trans. Met. Chem. 19 (1994) 265.
[47] R. Prabhakaran, P. Kalaivani, R. Huang, M. Sieger, W. Kaim, P. Viswanathamurthi, F. Dallemer, K. Natarajan, Inorg. Chim. Acta 376 (2011) 317.
[48] I. Fleming, Frontier Orbitals and Organic Chemical Reactions, Wiley, London (, 1976.
[49] N.H. Khan, E.A. Prasetyanto, Y.-K. Kim, M.B. Ansari, S.-E. Park, Catal. Lett. 140 (2010) 189.
[50] M.K. Choudhary, A. Das, R.I. Kureshy, M. Kumar, N.H. Khan, S.H.R. Abdi, H.C. Bajaj, Catal. Sci. Technol. 4 (2014) 548.
[51] W. Jin, X. Li, B. Wan, J. Org. Chem. 76 (2011) 484.
[52] T. Nitabaru, A. Nojiri, M. Kobayashi, N. Kumagai, M. Shibasaki, J. Am. Chem. Soc. 131 (2009) 13860.